AN UNDULATED SANDWICH PLATE WITH A NEW CORE

Anil Uzal, Fazil O. Sonmez*, Nuri Ersoy, and Kenan Cinar

Department of Mechanical Engineering, Bogazici University, Istanbul, Bebek 34342, Turkiye
*Email: sonmezfa@boun.edu.tr, Web Page: http://web.boun.edu.tr/sonmezfa/

Keywords: Sandwich panels, composite materials, acoustic emission, three-point bending, finite element modeling

Abstract
In this study, a new core design is introduced for sandwich composite structures. Its failure behavior is investigated via three-point bending tests. E-glass-fiber-reinforced epoxy resin is selected as the material for both the core and the face sheets. Acoustic emission (AE) method is used to detect the progression of damage. By carrying out fast Fourier transform of AE data, elastic waves caused by activated damage mechanisms are investigated in frequency domain in order to identify the corresponding failure modes. A finite element model of the sandwich structure is developed to predict the failure behavior of the specimens under the loading conditions in the tests. A promising agreement between the results of the finite element model and the experiments is observed. The deflection-force relation as well as the region where damage initiates are accurately predicted.

1. Introduction

For engineering applications, achieving an effective structural design is one of the major goals of the design stage. These structures are desired to be as light as possible and damage tolerant with high stiffness and strength properties. In some cases, the desired properties may be achieved by using monolithic composites while for some other applications, combining two different types of materials into one discrete structure like hybrid and sandwich composites leads to improved properties in terms of cost and weight. Sandwich structures are usually preferred for weight-critical applications requiring high flexural stiffness and strength. Face sheets are usually made of continuous fiber-reinforced composites or metals to impart high stiffness and strength, whereas core is a lightweight structure, which can be honeycomb, foam, corrugated, or truss structure. Separation of skins by placing a core between them increases the moment of inertia, which increases stiffness and reduces stresses. Each core structure possesses different mechanical and physical characteristics, which make them suitable for different types of application.

Stiffness and strength are the most important properties of sandwich structures that should be considered in design together with weight and cost. Load-displacement curves of tested specimens may give some clues regarding the activated failure modes. Besides examining the changes in the stiffness of specimens, a number of researchers also studied acoustic emission signals generated due to activated damage mechanisms to identify the activated failure modes of laminated composites with fiber-reinforced polymer matrix structures [1-3]. The majority of these researchers have focused on the amplitude parameter. Aramugam et al. [1] found that the peak frequency ranges 90-110 kHz and 130-200 kHz were related to matrix cracking and delamination for glass-epoxy laminates, respectively, while the range between 230-250 kHz was a sign of debonding; higher frequency content was observed during fiber failures. Bussiba et al. [2] considered counts rate and cumulative counts to identify failure modes. Asokan et al. [3] claimed that evaluating acoustic emission (AE) data according to amplitude and duration parameters might help to identify failure modes.

Excerpt from ISBN 978-3-00-053387-7

In this study, a new core design is introduced. The core has a truncated pyramidal shape with a square base as depicted in Figure 1. It is composed of fiber-reinforced composite layers similar to the skins. Thickness and orientation of the layers, the size of the unit cell, the core depth, and the wall angle define the geometric features of the core. It is possible to obtain numerous geometrical configurations by changing these parameters. One may optimize the geometric features for different loading conditions. The space may also be filled with foam to improve some physical properties for specific applications. Although this type of sandwich structure is more costly compared to honeycomb and foam core sandwiches, it is expected to show superior performance in the presence of transverse concentrated or distributed loads and shear loading. Unlike honeycomb cores, it can resist out-of-plane shear forces thanks to the angulated side faces and large contact surfaces. As opposed to corrugated ones, it provides high bending stiffness and strength in all directions not only in one direction.

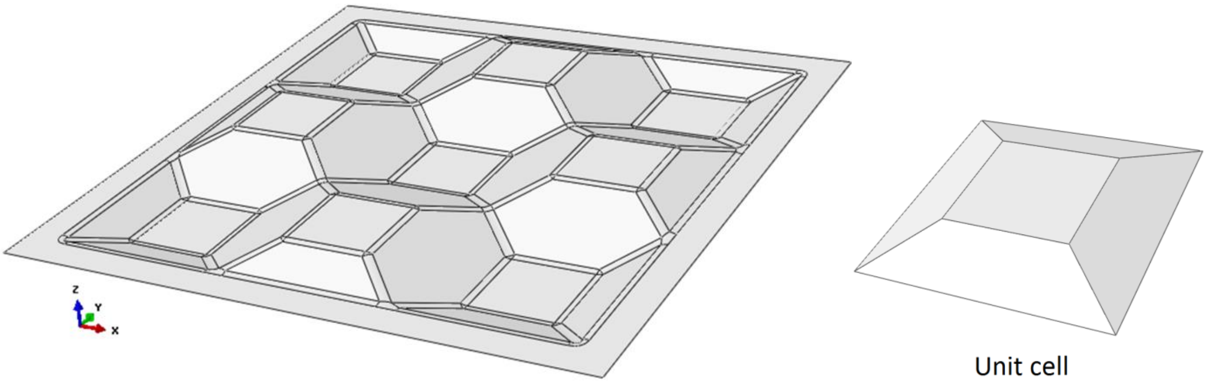

Figure 1. The schematic representation of the core design introduced in this study and unit cell.

The goal of this study is to investigate the strength and failure behavior of the undulated sandwich plate with the new core design under out-of-plane loading conditions by carrying out three-point bending tests and simulating the test by developing a finite element model to predict its mechanical response under loading.

2. Preparation of Specimens

In this study, E-glass fiber is chosen as the reinforcement material and epoxy is chosen as the resin material. For material properties see reference [4]. Sandwich composite specimens used in the tests are produced by vacuum infusion process (VIP). Both the core and the face sheets of the sandwich structure are composite laminates themselves. A properly cleaned thick glass is used to manufacture two face sheets and a three dimensional mold is used for the core. The mold shown in Figure 2 is made of RenShape®. Separately consolidated core and face sheets are bonded to each other by applying ARALDITE® 2000+ adhesive. They are held under press for at least 12 hours in order to obtain high bonding quality. Three sandwich plates are tested using the three-point bending test setup shown in Figure 3. The core and the face sheets are quasi-isotropic; their stacking sequence is $[0/45/-45/90]_s$. The thicknesses of the core and the face sheets are measured to be 1.40 mm and 1.20 mm, respectively. Accordingly, their ply thicknesses are taken as 0.175 mm and 0.15 mm, respectively. The three circular bars used in the fixture have a length of 300 mm and a diameter of 26 mm. For specimen 1, both of the piezoelectric transducers are placed on the top and no rubber bands are placed between the bars and the specimen. For specimens 2 and 3, one of the piezoelectric transducers is placed on the top and the other is placed on the bottom of the specimen and rubber bands are placed between the bars and the specimen. The test is displacement controlled with the rate of 3.55 mm/min.

Excerpt from ISBN 978-3-00-053387-7

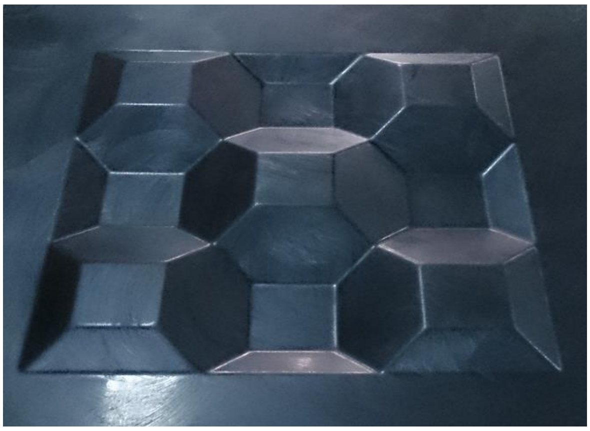

Figure 2. The lacquer coated mold for the core.

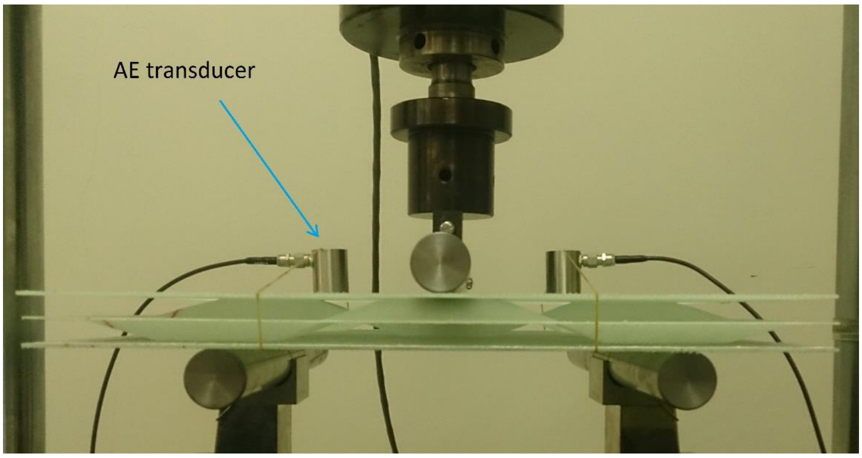

Figure 3. The three-point-bending test setup.

4. Finite Element Analysis

In order to predict the failure load and stiffness of the sandwich structure under three-point bending, an explicit finite element model is developed using ABAQUS finite element software. The face sheets and core are modeled separately and assembled together. The boundary conditions of the model reflect the physical loading conditions in three-point bending tests. The predicted region of failure, the deflection at which failure occurs, and the corresponding reaction force are compared with the physical test results in order to validate the model. The base area of a unit cell of the core structure, which is depicted in Figure 1, is 100 mm to 100 mm and the top area is 50 mm to 50 mm. In the specimens, nine of these unit cells are placed next to each other to create a 3 x 3 core structure. However, before merging these cells into a single part, four of them are flipped over. The height of a single cell is 10 mm, which means the core thickness is 20 mm from top to bottom. After merging, fillets with 5-mm radius of curvature are introduced and an outer frame is added as shown in Figure 1. Then, shell elements are generated through the surface. Additionally, 3D circular bars are created as rigid parts. A model of 3-mm-thick rubber band is also created between the rigid bars and the face sheets using 3D deformable solid elements. In the test specimens, the core is attached to the top and bottom faces using an adhesive. In order to avoid difficulties of modeling a very thin layer, the adhesive is not included in the finite element model. The interaction surfaces where adhesive is applied are simply tied to each. Contact properties between the bars and the part are defined as frictionless for tangential behavior and “hard-contact” for normal behavior. In order to fix the rigid

Excerpt from ISBN 978-3-00-053387-7

bars contacting the bottom of the sandwich plate, all displacement degrees of freedom are set to zero. The motion of the rigid bar at the top is only allowed in the transverse direction, U3, and it is set to 8 mm. In the face sheets, S4R elements are generated. S8R element type is used in the core part. Based on a mesh convergence analysis, the element sizes for the core and sheets are selected as 4 mm and 5 mm, respectively. Figure 4 shows the meshed assembly.

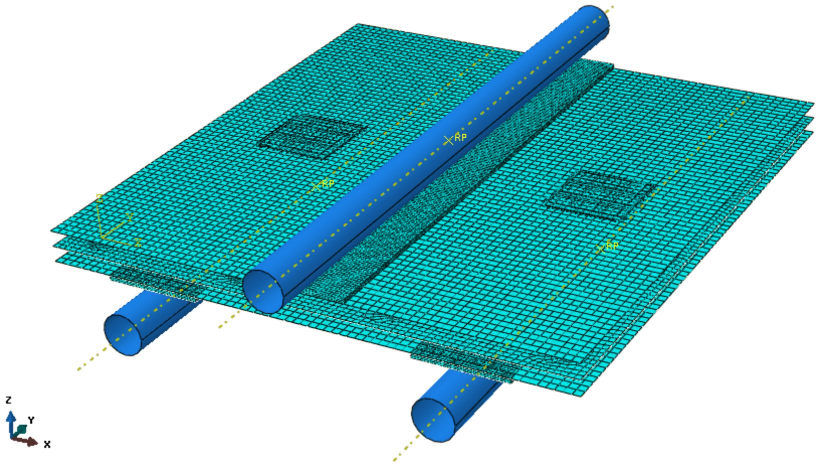

Figure 4. FE model of three-point bending and meshed assembly.

5. Three-Point Bending of the Sandwich Plates

In order to observe the failure behavior of the new sandwich design and verify the finite element model, three sandwich plates are manufactured and tested using a three-point bending test setup.
The tests are planned such that the load is increased until significant damage occurs in the plates. As seen in Figure 5, the plate keeps its integrity although the deflection at the end of the experiment exceeds almost three times its total thickness. At the peak load, the measured reaction force reaches 4820 N; the corresponding deflection is measured as 5.70 mm. For the other two specimens, the peak loads are measured to be 4430 N and 4650 N. Because 3-mm-thick rubber bands are used in the other tests, the corresponding displacements are larger, which are measured as 8.62 mm and 9.67 mm. The rubber bands are used in the other tests to reduce stress concentration and prevent generation of AE signals due to sliding between the bars and specimen.

Figure 6 shows the change in the load with the displacement of the middle bar and the corresponding peak frequency of AE data. Up to 3 kN, the load increases linearly, then the slope of the curve decreases up to the ultimate load level. The decrease in stiffness between 3.0 kN - 4.8 kN can partially be explained by the effects of activated failure mechanisms, because AE equipment starts to detect signals above 3 kN. The peak frequencies lie in the same frequency bands as the tension tests. Load-displacement curve is also linear between 3.0 kN and 3.7 kN, but with reduced stiffness and peak frequency of AE hits indicate matrix related damage mechanisms, which are matrix cracking corresponding to 130-170 kHz band and fiber-matrix debonding corresponding to 220-260 kHz band. The curve is linear between 3.7 kN and 4.1 kN; in this range fiber-related signals are also detected, which are about 350 kHz. Above 4.1 kN, the number of AE signals rapidly increases and stiffness continually decreases until the ultimate load level. After the ultimate load level is reached, discontinuities in the curve are observed accompanied by high numbers of AE hits with frequencies indicating occurrence of all failures modes. Peak frequencies in 180-200 kHz band, which indicate delamination, are detected in significant number only after the ultimate load level is reached. After

Excerpt from ISBN 978-3-00-053387-7

that, the load bearing capacity of the plate decreases; however it can still withstand loads above 2.5 kN until the deflection reaches 18 mm (Figure 5.a).

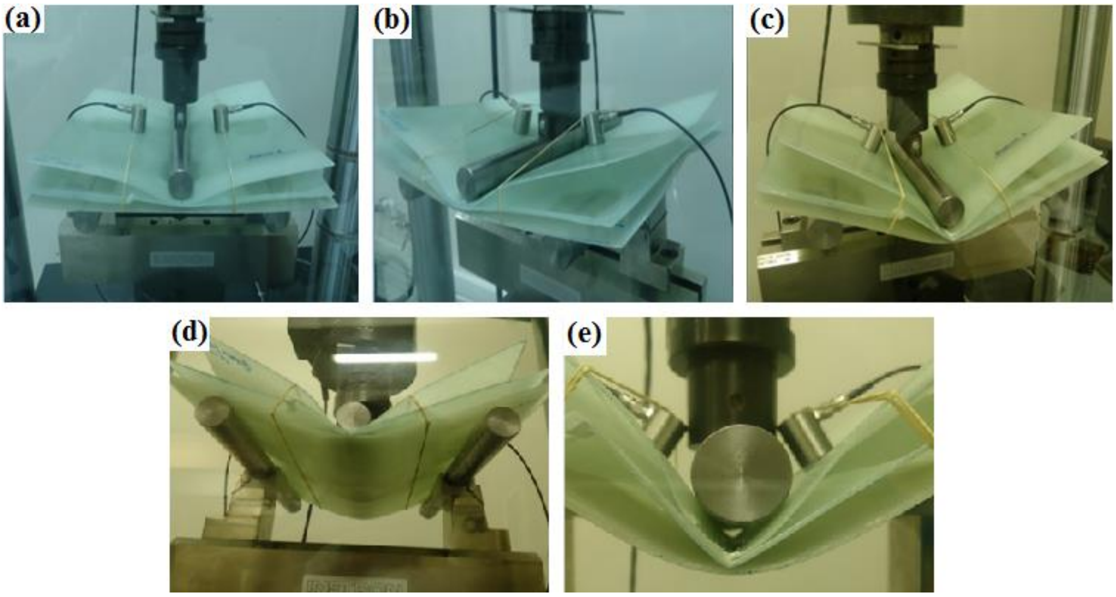

Figure 5. Three-point bending test depicted at the stage when the deflection of the middle bar is (a) 17 mm, (b) 28 mm, (c) 52 mm (d) 52 mm, and (e) 66 mm.

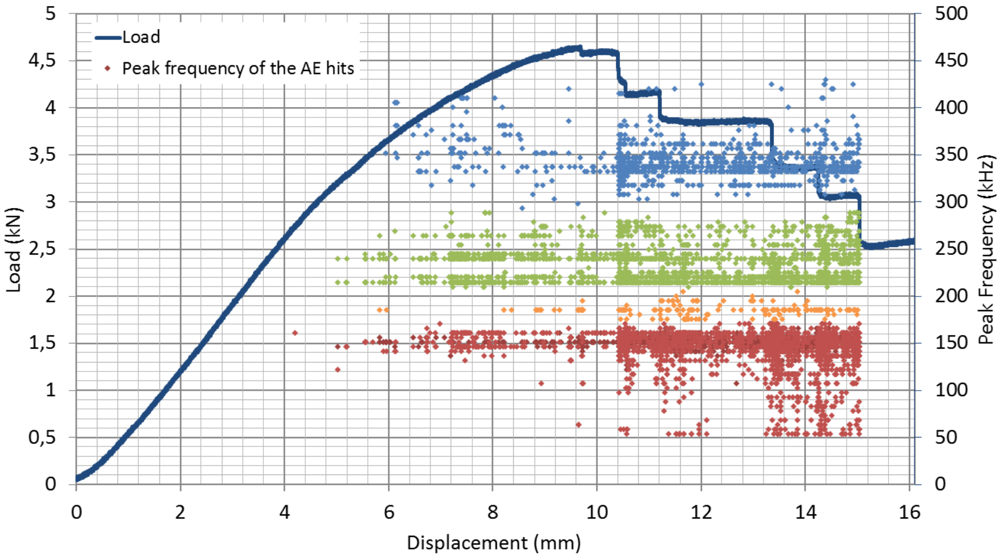

Figure 6. Peak frequency distribution of AE hits and load vs. strain for a sandwich specimen under three-point bending.

In order to verify the finite element model, the loading conditions up to the peak load level are considered. In order to predict the failure behavior after the plate undergoes substantial damage, a progressive model has to be developed, which is not within the scope of this study. The structural model with rubber bands is subjected to deflection controlled loading by setting the displacement of the middle bar, U3, to 8 mm. The maximum in-plane principal stress state in the top layer of the core is shown in Figure 7. The fibers are oriented in the *x* direction. There is stress concentration at the edges of the core, where initial damages are expected to occur.

Excerpt from ISBN 978-3-00-053387-7

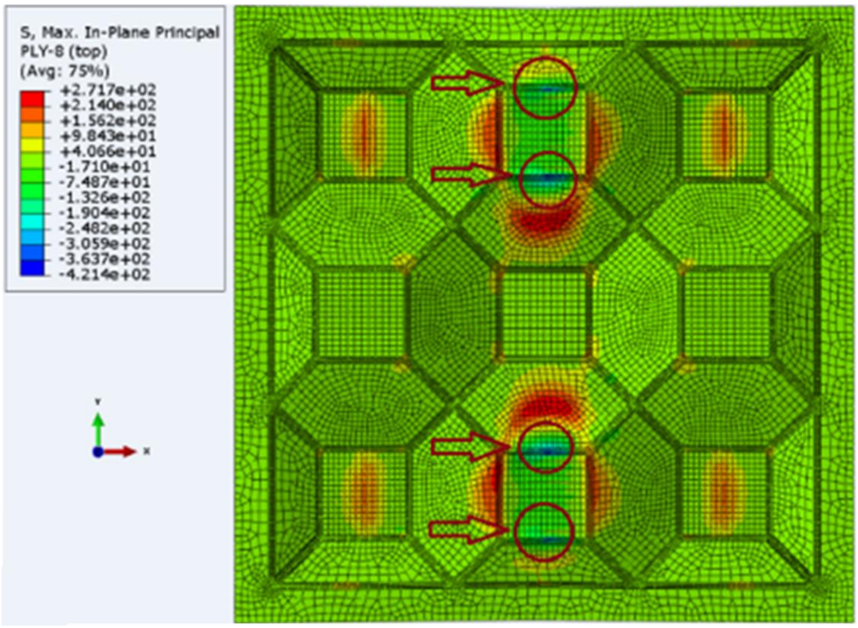

Figure 7. The maximum in-plane principal stress state distribution in the core corresponding to 8-mm displacement.

Figure 8.a shows Tsai-Hill failure index distribution in the middle layer of the core, where fibers run in the y direction. The edges of the core naturally cause stress concentration. In Figure 8, 1.0 is selected as the upper limit. In the grey regions, the failure index is above 1.0, therefore they are assumed to have failed. The first specimen is cut into two pieces for inspection. Comparing the distribution of the failure index predicted by the FE model in Figure 8 and the failed regions in the specimen shown in Figure 8.b, one may infer that the agreement between the model predictions and the test results is quite satisfactory

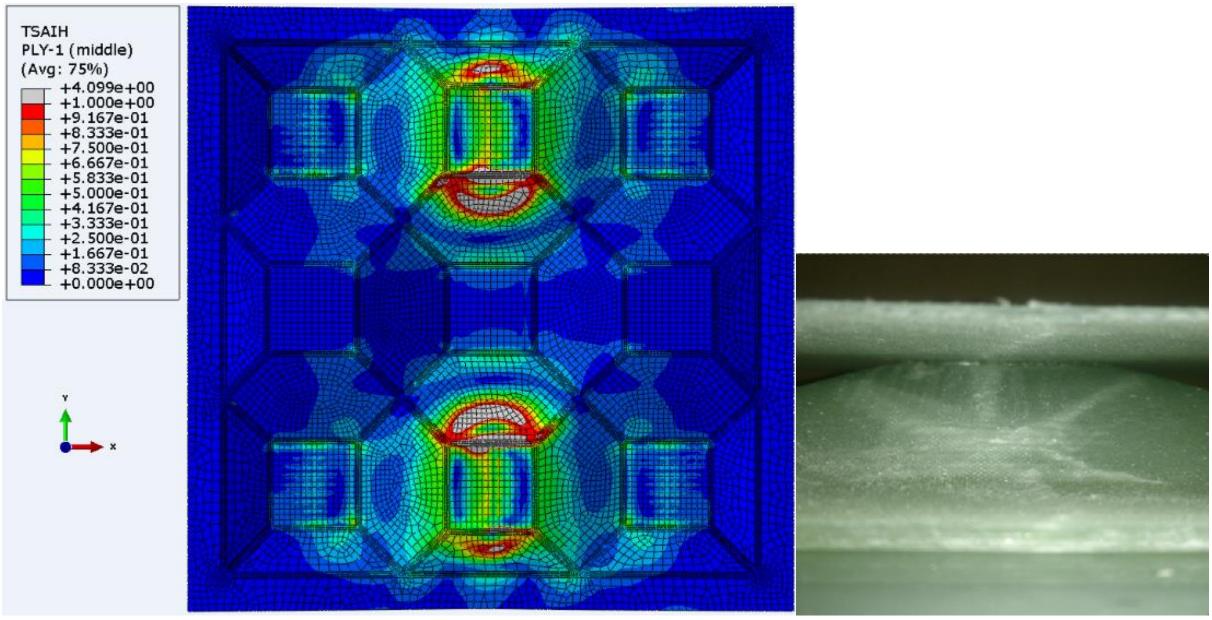

Figure 8. (a) The failure index distribution of the core. (b) The damaged region in the core.

Excerpt from ISBN 978-3-00-053387-7

A Python Script code is developed and an iterative study is conducted using Secant algorithm to estimate the failure load, at which the maximum failure index is equal to one. If the regions with excessive stress concentration are included in the failure assessment, the FE model highly underestimates the failure load. Considering that the top surfaces of the cores are rigidly attached to the face sheets, while in reality, the connection is not rigid and the edges of the glued region are not sharp, the predicted stresses in this region are expected to be more severe than the actual stresses both in the face sheet and the core. This is one of the reasons of underestimating the strength. Secondly, initial damages that occur locally at stress concentration regions hardly effect the macro behavior of the structure. Because of these reasons, the severely stress concentrated regions are neglected in the strength assessment procedure. There are two cells of the core on the *y-z* symmetry plane which are directly attached to the top face sheet and there are two edges parallel to the *x*-direction for each cell, where stresses are locally high. Between the glued surfaces and the angulated core walls, the curved fillet regions exist. Tsai-Hill failure index values at all the elements on these four fillets and the first rows of the elements at the two sides of these regions are not taken into account. Similarly, the elements of the top face sheet which lie within the vertical projection of the neglected areas of the core are also not taken into account. After seven iterations, the algorithm finds that the initial failure occurs at the top layer of the core when the deflection of the middle bar is 5.91 mm. Corresponding reaction force is obtained to be 4590 N. The initial failure occurs at an angulated core wall. In the most critical element, where Tsai-Hill failure index is equal to 1.0, the transverse stress is 73.9 MPa, which is close to the transverse tensile strength of the composite material, while the other stress components in principal material directions are much lower than their respective strengths. Therefore, one may conclude that the predicted first-ply failure mode is matrix failure. The FE model results reveal that tensile stresses develop in the top layer of the core in the critical region, while compressive stresses develop in the bottom layer, which means that the wall of the core buckles outward. This implies that local buckling in the core is one of the failure mechanisms. The nonlinearity in the load-displacement curve of the sandwich plate (Figure 6) may partially be attributed to local buckling beside damage progression. In the tests where rubber bands are used, the force on the bar corresponding to the deflection of 5.91 mm is measured to be 3720 N in one specimen and 3630 N in the other. As seen in Figure 6, the AE setup starts to detect significant acoustic waves at 5.91-mm deflection with peak frequencies indicating matrix damage. Although the predicted failure load (4590 N) is about 20% higher than the measured level, the prediction of the region where the initial failure occurs, the mode of failure, and the prediction of the corresponding deflection are successful.

Figure 9 shows the load vs. deflection curves of the FE model of the sandwich specimens, and the test data for the second and third specimens. The agreement between the results of the FE model and the actual mechanical response of the sandwich structure is acceptable. Even though linear material properties are used and progression of damage is not taken into account in the FE model, nonlinear mechanical response of the plate due to local buckling is predicted by the model. In order to estimate the gain in stiffness by introducing the new core design, a plain laminated plate with the same lamina thicknesses and stacking sequence is also modeled. The equivalent plate has 24 plies with the same stacking sequence $[0/45/-45/90]_{3s}$ and its thickness is equal to 3.84 mm. The FE model of the plain laminate with equivalent use of material is subjected to the same loading conditions. As seen in Figure 9, although the sandwich structure has almost the same weight with the equivalent plate, its stiffness is approximately 4.5 times the equivalent plate's stiffness.

6. Conclusions

In this study, the failure behavior of an undulated sandwich plate with a new core design is investigated. E-glass-fiber-reinforced epoxy is selected as the material of the structure. In order to understand the failure behavior under out-of-plane loading, sandwich laminates are manufactured with dimensions of 340 × 340 × 20 mm and tested using a three-point bending setup under real-time acoustic emission monitoring. The collected AE data are post-processed and classified according to their dominant frequency characteristics. It is found out that under transverse forces, the sandwich

Excerpt from ISBN 978-3-00-053387-7

plates with the unique core design can withstand loads up to 5 kN. This unique design has a linear response up to 3 kN, which is followed by matrix cracking, fiber-matrix debonding, and local buckling of core faces. In the deflection controlled experiments, after leaving the peak load level behind, the structure is observed to withstand further deformation without catastrophic failure. After some point, extensive fiber failures are observed; still the part can carry 1.8 kN load even after vertical deflection exceeds three times the plate thickness. To predict the failure behavior of the sandwich plate, a parametric Python Script code is developed to model the structure and simulate three-point bending tests. As the failure measure, Tsai-Hill failure criterion is adopted. The failure load is found iteratively using the secant algorithm and the outcome is compared with the experimental results. The region of failure, mode of failure, and the deflection at which failure initiates are correctly predicted. Structural design optimization of the core and comparison of the new sandwich design with conventional sandwich designs like corrugated and foam filled sandwiches are left as future studies.

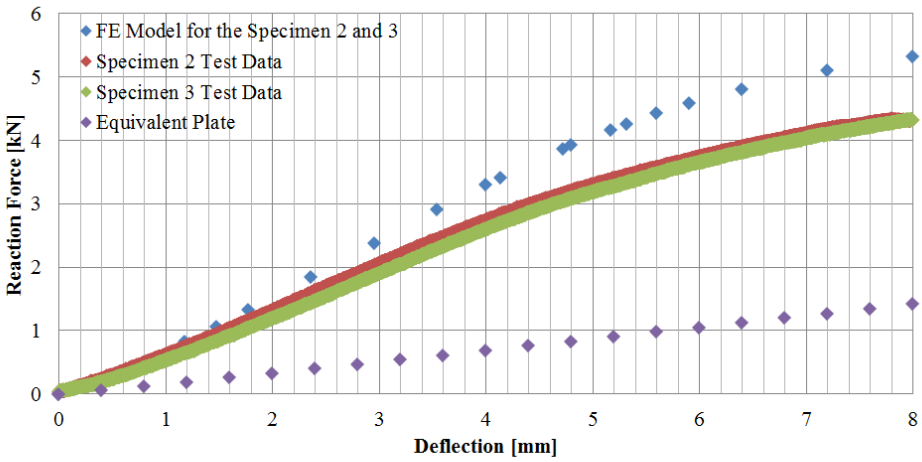

Figure 9. Load vs. middle bar deflection curves for the FE model of the sandwich specimens, the test data for the 2nd and 3rd specimens and the FE model of an equivalent plate.

Acknowledgments

This paper is based on the study supported by the Scientific Research Projects of Bogazici University with the code number 11168-16A06P2. The authors would also like to thank to Istanbul Development Agency, which supported the development of the infrastructure of Composites Laboratory in Bogazici University under project code ISTKA/BIL/2012/58.

References

[1] V. Aramugam, S.B. Kumar, C. Santulli, and A.J. Stanley. Effect of fiber orientation in uni-directional glass epoxy laminate using acoustic emission monitoring. *Acta Metallurgica Sinica*, 24:351-364, 2011.

[2] A. Bussiba, M. Kupiec, S. Ifergane, R. Piat, and T. Böhlke. Damage evolution and fracture events sequence in various composites by acoustic emission technique. *Composites Science and Technology*, 68:1144-1145, 2008.

[3] R. Asokan, V. Aramugam, C. Santulli, S.B. Kumar, A.J. Stanley. Investigation of the strength of the failure modes in GFRP laminates using acoustic emission monitoring. *International Journal of Polymers and Technologies*, 3(2): 57-65, 2011.

[4] A. Uzal, *Failure behavior of undulated sandwich plates under out-of-plane loading*, Bogazici University M.S. Thesis, 2014.